HOKKAIDO UNIVERSITY

Title	Growth Kinetics of Elementary Spiral Steps on Ice Prism Faces Grown in Vapor and Their Temperature Dependence
Author(s)	Miyamoto, Genki; Kouchi, Akira; Murata, Ken-ichiro et al.
Citation	Crystal growth & design, 22(11), 6639-6646 https://doi.org/10.1021/acs.cgd.2c00851
Issue Date	2022-10-05
Doc URL	https://hdl.handle.net/2115/90510
Rights	This document is the Accepted Manuscript version of a Published Work that appeared in final form in Crystal Growth & Design, copyright c American Chemical Society after peer review and technical editing by the publisher. To access the final edited and published work see https://pubs.acs.org/articlesonrequest/AOR-U6VTEIQUPB2XAFJFIBVZ.
Type	journal article
File Information	16 Manuscript_Miyamoto_Sazaki.pdf

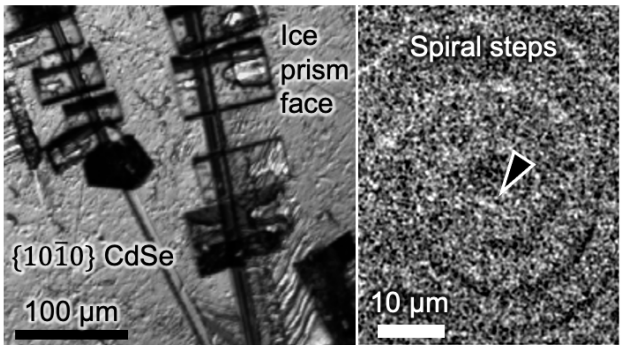
Hokkaido University Collection of Scholarly and Academic Papers : HUSCAP

Growth kinetics of elementary spiral steps on ice prism faces grown in vapor and their temperature dependence

Genki Miyamoto[1], *Akira Kouchi*[1], *Ken-ichiro Murata*[1], *Ken Nagashima*[1], *Gen Sazaki*[1,*]

[1] Institute of Low Temperature Science, Hokkaido University, N19-W8, Kita-ku, Sapporo 060-0819, Japan

Abstract.



We grew ice prism faces heteroepitaxially on a CdSe wafer. Then we measured lateral growth velocity of elementary spiral steps on the ice prism faces, for the first time, by advanced optical microscopy. We determined the temperature dependence of a step kinetic coefficient at temperatures from -25.0 to -2.6 °C.

* To whom correspondence should be addressed. E-mail: sazaki@lowtem.hokudai.ac.jp

Growth kinetics of elementary spiral steps on ice prism faces grown in vapor and their temperature dependence

Genki Miyamoto[1], *Akira Kouchi*[1], *Ken-ichiro Murata*[1], *Ken Nagashima*[1], *Gen Sazaki*[1,*]

[1] Institute of Low Temperature Science, Hokkaido University, N19-W8, Kita-ku, Sapporo 060-0819, Japan

KEYWORDS: elementary spiral step, prism face, ice crystal, step kinetic coefficient, step ledge free energy, temperature dependence, advanced optical microscopy

[*] To whom correspondence should be addressed. E-mail: sazaki@lowtem.hokudai.ac.jp

ABSTRACT (179 < 200 words)

We grew prism faces of ice crystals heteroepitaxially on a $\{10\bar{1}0\}$ CdSe wafer. Then we observed the lateral growth of elementary spiral steps on prism faces in vapor by advanced optical microscopy. On prism faces, we found that outcrops of screw dislocations are mostly located in the interiors of prism faces and that distance L between adjacent spiral steps is uniform, whereas these two features are not observed on basal faces. We measured the velocity V_{step} of elementary spiral steps on prism faces under various supersaturation and determined the step kinetic coefficient β. Then we revealed that the value of β on prism faces monotonically decreases with decreasing temperature (T) from -2.6 to -25.0 °C. In this T range the value of β on prism faces is significantly smaller than that on basal faces (determined previously). We further analyzed the relation between L and driving force for crystallization $\Delta\mu$ and found that at $T \sim$ -15 °C step ledge free energy κ on prism faces reaches a peak (8.5×10^{-10} J/m), implying the change in surface structures at this temperature.

1. INTRODUCTION

Ice is one of the most abundant materials on the earth's surface. Therefore, its phase transitions govern a wide variety of natural phenomena. Rainfall and snowfall are phase transitions of ice themselves.[1] Reflection of sunlight on ice sheets significantly influences global temperature.[2] In addition, the fluctuation in the volume of ice crystals in the cryosphere changes the sea level.[3] Hence, the quantitative understanding of the growth kinetics of ice crystals is crucially important for understanding such natural phenomena.

Many studies have been so far carried out to observe the growth of ice crystals mainly by optical techniques. Ordinary bright-field optical microscopy[4-6] and differential interference contrast microscopy[7-14] were used to measure the size of ice crystals and surface morphologies such as bunched steps, respectively. Two-beam interferometry[15-20] enabled the precise measurements of normal growth rate at several-nm/s level and three-dimensional surface topography of ice crystals. However, none of these optical techniques could visualize elementary steps on ice crystal surfaces, mainly because of small detection sensitivity in the height direction. In order to overcome such difficulty, we and Olympus Engineering Co. Ltd. have developed laser confocal microscopy combined with differential interference microscopy (LCM-DIM).[21] Utilizing significant noise reduction function of LCM and a three-dimensional-like contrast of DIM, we could successfully visualize individual elementary steps (0.37 nm in thickness) on basal faces of ice crystals grown in vapor.[22] Although LCM-DIM has a disadvantage of a slow image-acquisition rate (several s for an image of 1,024 x 1,024 pixels), LCM-DIM is a powerful tool for studying the growth kinetics of ice crystals at the elementary step level.

After achieving the in-situ observation of elementary steps, we performed a series of studies of elementary spiral steps on basal faces of ice crystals,[23-26] which were heteroepitaxially grown

on a cleaved AgI crystal. Then we found that spiral steps on basal faces exhibit a double-spiral pattern,[23] which can be expected from ice's crystallographic structure. In addition, we revealed that on ice basal faces outcrops of screw dislocations are always located at the edges of basal faces and that distance L between adjacent spiral steps shows a significantly large variation.[24] We could also successfully measure the lateral velocity V_{step} of elementary spiral steps on ice basal faces and confirmed that surface diffusion of water admolecules on basal faces plays a crucially important role in the growth kinetics of elementary spiral steps.[25] In addition, we also determined the step kinetic coefficient β of elementary spiral steps on basal faces from the supersaturation dependence of V_{step}, and discovered that β on basal faces exhibits complicated temperature dependence.[24]

In contrast to the studies of elementary steps on ice basal faces, those on ice prism faces, which are another important facet of ice crystals grown in vapor, are still very preliminary, because of the experimental difficulty in the reproducible preparation of prism faces that are perpendicular to an optical axis. To prepare such prism faces, the use of a heteroepitaxial substrate crystal is indispensable. So far there has existed a study that reported the heteroepitaxial growth of ice prism faces on crystals of several kinds of steroids[27]. However, probably because steroids have complicated molecular structures and are not common, the steroid crystals were not utilized as heteroepitaxial substrates of ice prism faces. Therefore, we tried to find a substate crystal which is more common and easy to use for the heteroepitaxial growth of ice prism faces. As such a substrate crystal, we examined a prism face of a CdSe crystal, because both CdSe and ice crystals have the Wurtzite structure and close lattice constants (CdSe: $a = 0.430$ nm and $c = 0.702$ nm[28], and ice: $a = 0.452$ nm and $c = 0.736$ nm[29]).

In this study, we grew ice crystals heteroepitaxially on a prism face of a CdSe crystal and studied the growth kinetics of ice prism faces at the elementary-step level, for the first time.

We measured the lateral velocity V_{step} of elementary spiral steps on ice prism faces by LCM-DIM. From the dependence of V_{step} on supersaturation σ, we determined the step kinetic coefficient β on prism faces. We performed similar experiments in a temperature (T) range from -25.0 to -2.6 °C and revealed the T dependence of β. In addition, from the relation between the distance L between adjacent spiral steps and the driving force for the crystallization $\Delta\mu$, we discussed the T dependence of step ledge free energy κ.

2. EXPERIMENTAL PROCEDURES

Our custom-built observation chamber was made of two Cu plates (Fig. S1 in the supporting information). The temperatures of upper and lower Cu plates, T and T_{bottom}, were separately controlled using Peltier elements. At the center of the upper Cu plate, a $\{10\bar{1}0\}$ CdSe wafer (purchased from MTI Corporation, USA) was attached as an ice-nucleating substrate (the CdSe wafer was cut into a piece of 3 x 3 mm^2, and the surface of the wafer was scratched using a glass cutter just before the experiment to expose fresh CdSe surfaces). Sample ice crystals were grown heteroepitaxially on this CdSe substrate. On the lower Cu plate, ice crystals were also grown to supply water vapor to the sample ice crystals for the observation. The total pressure in the observation chamber was kept at atmospheric pressure by filling the chamber with pure nitrogen gas. The volume of the ice crystals for supplying water vapor was significantly larger than that of the sample ice crystals. Hence, the partial pressure of water vapor P in the observation chamber was determined by T_{bottom}. In addition, the equilibrium partial vapor pressure P_e of the sample ice crystals was determined by T. The supersaturation of the water vapor, $\sigma = (P - P_e)/P_e$, was adjusted by changing T_{bottom} and T. The values of P and P_e showed

errors of ±0.5 Pa, respectively; hence, σ exhibited an error of ±0.001. Details of the chamber and its operation are explained elsewhere.[22, 24]

The sample ice crystals were observed using a laser confocal microscope combined with a differential interference contrast microscope (LCM-DIM):[21, 22] a laser confocal system (Olympus Corp., model FV300) was combined with an inverted optical microscope (Olympus Corp., model IX70). An objective lens with 10× magnification was used with the LCM-DIM. A super luminescent diode (Amonics Ltd., model ASLD68-050-B-FA), whose wavelength and coherent length were 680 nm and 10 μm, respectively, was used as a light source. The LCM-DIM can provide three-dimensional contrast to subnanometer-height steps on flat crystal surfaces.[22] The differential interference contrast was adjusted as if an ice crystal surface were illuminated by a light beam slanted from upper to lower direction. Thus, as shown in Fig. 2, a convex object exhibited brighter and darker contrasts on the upper and lower sides of the object, respectively.

To investigate the intrinsic growth kinetics of elementary steps at a certain T, a step kinetic coefficient β was evaluated. It is well-known that the lateral velocity of elementary steps V_{step} is proportional to supersaturation on a crystal surface $\sigma_{\mathrm{surf}} = (P_{\mathrm{surf}} - P_{\mathrm{e}})/ P_{\mathrm{e}}$: here P_{surf} is the partial pressure of water vapor on a crystal surface.[30, 31] When σ is very small, $\sigma_{\mathrm{surf}} \sim \sigma = (P - P_{\mathrm{e}})/ P_{\mathrm{e}}$. Therefore, at $\sigma \sim 0$, we obtain

$$V_{\mathrm{step}} \equiv \beta \frac{P_{\mathrm{surf}} - P_{\mathrm{e}}}{P_{\mathrm{e}}} \cong \beta \frac{P - P_{\mathrm{e}}}{P_{\mathrm{e}}} = \beta\sigma. \qquad (1)$$

To determine the temperature dependence of β, V_{step} was measured as a function of σ at temperatures T ranging from -25.0 to -2.6 °C.

3. RESULTS AND DISCUSSION

3.1. Temperature dependence of the step kinetic coefficient β. We first investigated the capability of a $\{10\bar{1}0\}$ CdSe surface to act as a heteroepitaxial substrate of ice prism faces. Figure 1 shows photomicrographs of a surface of a CdSe substrate 10 min. after we made water vapor in the observation chamber supersaturated. White and black arrowheads present scratches that we intentionally made, using a glass cutter, just before and 7-days before the experiment, respectively. As shown in Fig. 1a, ice crystals were formed only on these scratches. In addition, note that the number of ice crystals formed on the new (white arrowheads) and 7-days-old (black arrowheads) scratches were 36 and 1 (marked by the white arrow in Fig. 1a), respectively (regarding the ice crystal marked by the white dotted arrow, see the caption of Fig. 1). These results indicate that the nucleation activity of the CdSe substrate decreases significantly as time elapsed. Among the 36 crystals formed on the new scratches, 17 crystals (46 %) exhibited a rectangular shape and the same orientation (as the crystal marked by the black arrow). Such rectangular and oriented ice crystals demonstrate that prism faces of the ice crystals were heteroepitaxially grown on the $\{10\bar{1}0\}$ CdSe substrate. The absence of ice crystals on the unscratched surface probably indicates that the unscratched surface of the CdSe substrates was oxidized and hence inactive in the heterogeneous nucleation of ice crystals. As far as we examined, a $\{10\bar{1}0\}$ surface of CdSe is the first inorganic substrate for the heteroepitaxial growth of ice prism faces.

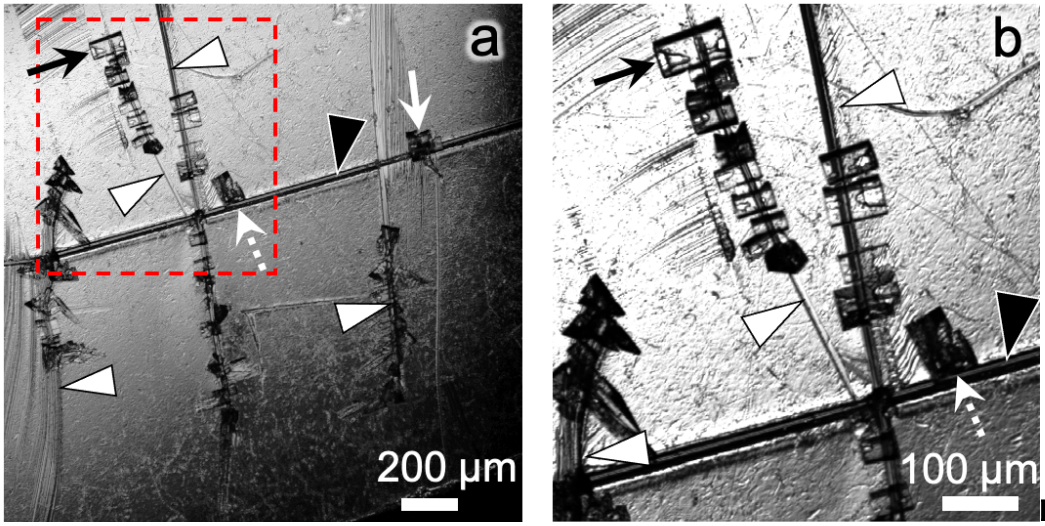


Fig. 1

We next observed elementary steps on prism faces grown on the CdSe substrate in-situ by LCM-DIM. Figure 2 shows a typical example of a prism face growing in vapor. The time-evolution of LCM-DIM images clearly demonstrates that the prism face was growing by the spiral growth mechanism in the supersaturation range adopted in this study ($\sigma \leq 0.12$). A black arrowhead indicates the location of a screw dislocation that induced the spiral growth. We found that on prism faces screw dislocations are mostly located in the interiors of crystal faces, whereas on basal faces screw dislocations are always located at the edges of ice crystals (see a black arrowhead shown in Fig. S2 in the supporting information).[24, 25] In addition, the distance L between adjacent spiral steps on a prism face looks almost uniform, in contrast to the large variation in L on a basal face (Fig. S2).[24, 25] On the prism faces formed on the $\{10\bar{1}0\}$ CdSe surfaces, there existed about 1~3 active dislocation outcrops in a 100-μm square.

In this study, we carried out our measurements at relatively small σ (≤ 0.12) to determine the values of β correctly (to avoid the depletion of water vapor in a vicinity of a prism face). Hence, in all measurements performed in this study, we could observe only the spiral growth on ice prism faces. However, in our previous study,[22] we could also observe the two-dimensional (2D)

nucleation growth on prism faces (such prism faces were obtained just by chance). We are planning to perform quantitative studies on 2D nucleation in the near future.

In Fig. 2, white arrowheads indicate the position of an identical step. We measured lateral velocity V_{step} of elementary spiral steps by tracking the time evolution of the position of the identical step. From the measurements of about five steps, we determined the average and standard deviation of V_{step} at certain T and σ. A movie of the process shown in Fig. 2 is available as Video S1 in the supporting information.

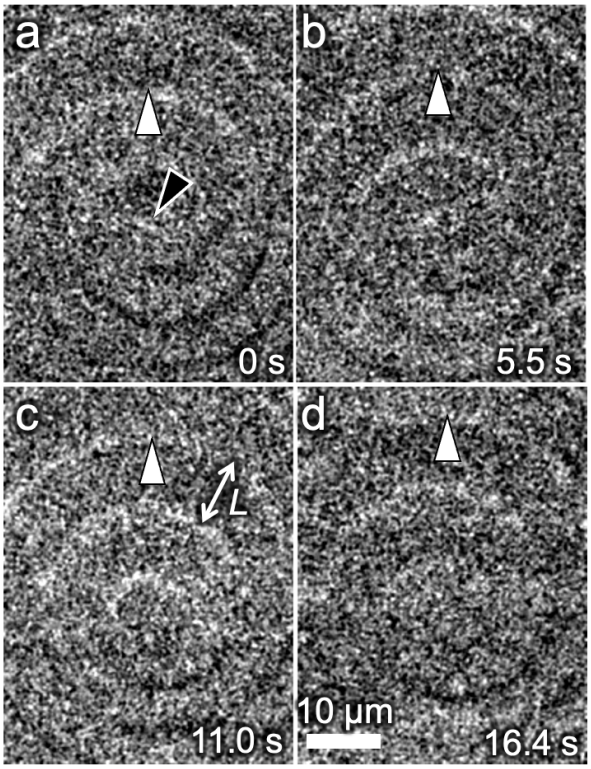


Fig. 2

In the temperature range from -25.0 to -2.6 °C, we measured V_{step} under various supersaturation σ. Figure 3 shows the summary of all data. At each T, to determine $\sigma = 0$ experimentally, we directly observed the forward/backward movement of elementary steps and the growth/sublimation of the edges of crystals, controlling P carefully. As shown in Fig. 3, the majority of the V_{step} vs. σ plots shows a linear relation. We fitted these experimental results using a linear function from the origin (solid straight lines) to determine the value of β. In

contrast, at T = -22.0, -22.3, and -25.0 °C °C, when σ became relatively large, the V_{step} vs. σ plot deviated from the linear relation and finally reached an asymptote, as also observed previously on basal faces.[24] This behavior arose from the depletion of water vapor in the vicinity of prism faces. In such cases, we fitted the data points using a hyperbolic tangent function (broken curves) and determined the value of β from the slope at $\sigma = 0$. With respect to the depletion of water vapor at lower temperatures, we will discuss at the end of this section.

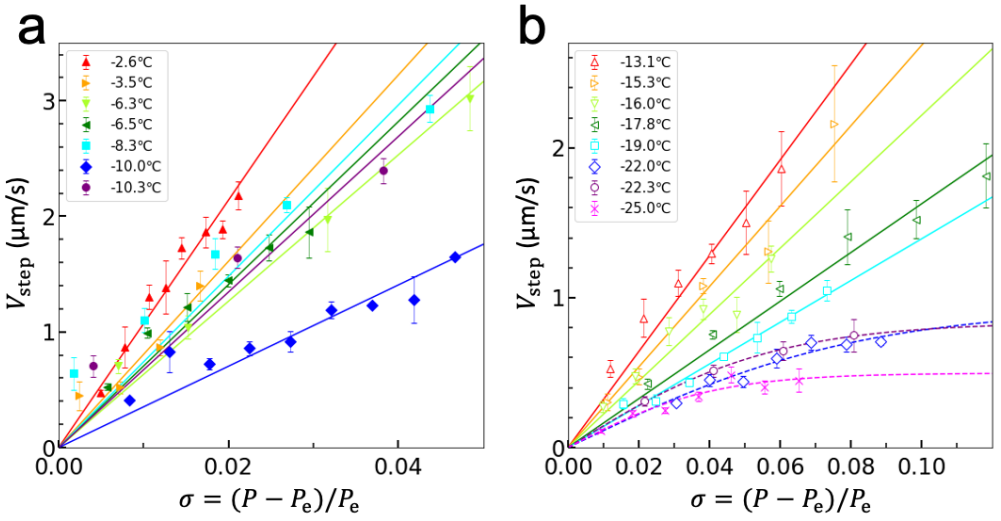


Fig. 3

Figure 4a shows the changes in β determined from Fig. 3 as a function of T. Filled squares show the values of β determined on prism faces in this study, whereas open circles present the values of β determined on basal faces previously.[24] As shown in Fig. 4a, on prism faces the values of β decreased monotonically with decreasing T, whereas on basal faces the values of β exhibited a more complex behavior.[24] From the viewpoint of T dependence, β on prism faces shows more normal behavior than that on basal faces. In the T range from -25.0 to -2.6 °C, the values of β on prism faces were significantly smaller than those on basal faces.[24] At present, the reason why the values of β on basal and prism faces show significant difference is still unclear. T dependence of surface structures of prism faces needs to be studied by surface-

sensitive methods, such as grazing-incidence (GI) diffractometry and sum frequency generation (SFG) spectroscopy in the future.

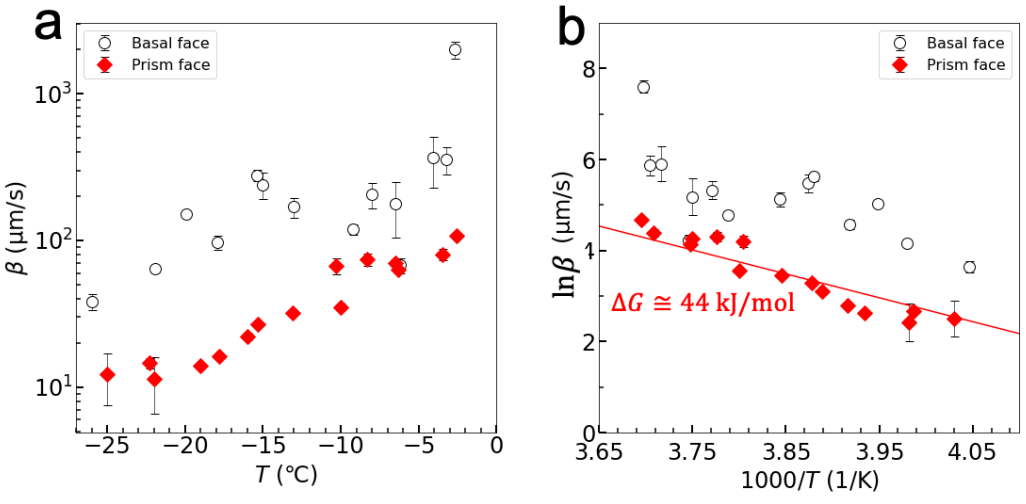


Fig. 4

From the T dependence of β, we can also obtain an activation free energy ΔG for the incorporation of a water molecule into a kink, using the following Arrhenius type equation:[30, 31]

$$\beta = a\nu \cdot \exp\left(-\frac{\Delta G}{k_B T}\right). \quad (2)$$

Here, a is the lattice constant (0.4 nm), ν is the molecular vibration frequency (4×10^{13} 1/s: Debye frequency of ice), and k_B is the Boltzmann constant. The straight line in Fig. 4b shows the results of the curve fitting using eq. (2). Although the variation of the filled plots is not so small, it would be scientifically sound to fit the data in Fig. 4b using single exponential function (eq. (2)). From the curve fitting, we obtained ΔG = 44 ± 1 kJ/mol. Because the value of 44 kJ/mol is close to the latent heat of the sublimation of ice (51 kJ/mol),[32] the analysis using eq. (2) looks plausible. In contrast, on basal faces the data roughly show the similar slope. However, at present, the complicated T dependence of β on basal faces is fully unclear. Therefore, we must leave the interpretation to future studies.

As shown in Fig. 3b, water vapor in the vicinity of a growing ice crystal was depleted at lower T. The depletion of water vapor occurs when the consumption of water vapor by the growth becomes larger than the supply of water vapor by volume diffusion. As shown in Fig. 4a, the decrease in T from 0.0 to -22.0 °C makes β one order smaller. Next let us estimate the changes in the flux of the volume diffusion J with decreasing T. For simplicity, we examine the case at relatively large σ, at which condition P_{surf} reaches P_e (note that J thus estimated corresponds to its maximum value). At such condition, J is expressed as follows:[30, 31]

$$J = -D\left.\frac{\partial P}{\partial z}\right|_{z=0} \cong -D\frac{P-P_e}{\delta}. \quad (3)$$

Here, D is the diffusion coefficient of water vapor, z is the distance from a crystal surface, δ is the thickness of a diffusion boundary layer. Although the precise estimation of δ is difficult, it is known that $\delta \propto D^{-1/2}$.[30, 31] Therefore, we obtain $D/\delta \propto D^{3/2}$. The decrease in T from 0.0 to -22.0 °C makes D 0.85 times smaller,[33] hence D/δ becomes $(0.85)^{3/2} = 0.78$ times smaller. In addition, considering P_e = 611 and 85.1 Pa at 0 and -22.0 °C,[34, 35] respectively, the decrease in T makes $(P - P_e)$ 0.14 times smaller when $\sigma = 0.05$. Therefore, J becomes at least 0.78 x 0.14 = 0.11 times smaller with decreasing T from 0.0 to -22.0 °C. Because the value of J estimated by eq. (3) shows its maximum value, we can expect that the flux of volume diffusion in our experiments was much smaller. Therefore, we can conclude that with decreasing T the decrease in J became larger than that in β, resulting in the more significant depletion of water vapor at lower T (Fig. 3b).

3.2. The distance L between adjacent spiral steps. We can experimentally determine the distance L between adjacent spiral steps by LCM-DIM (Fig. 2). As demonstrated in Figs. 2 and

S3a, L on prism faces shows a narrow distribution irrespective of σ, whereas L on basal faces showed a significantly wider distribution with decreasing σ (Figs. S2 and S3b). The reason for the strange behavior of L on basal faces is unfortunately still unclear. However, we can expect that the normal behavior of L on prism faces follows the Barton-Cabrera-Frank (BCF) theory.[36-38]

When σ is very small, L is large enough to avoid the competition of adjacent spiral steps for water admolecules diffusing on a terrace. Under such conditions, L can be expressed as[39]

$$L = 19\rho_c = 19\frac{s\kappa}{\Delta\mu_{surf}}. \quad (4)$$

Here, ρ_c is the radius of a critical two-dimensional nucleus, s is the area occupied by one water molecule (s = 8.30 x 10^{-20} m^2),[29] κ is the step ledge free energy, $\Delta\mu_{surf}$ is the driving force for the crystallization on a crystal surface ($\Delta\mu_{surf} = k_B T \ln P_{surf}/P_e$). When the V_{step} vs. σ plot (Fig. 3) shows a straight line, we can consider $P_{surf} = P$. However, when the V_{step} vs. σ plot deviates from the linear relation, water vapor in the vicinity of a growing prism face is depleted ($P_{surf} < P$). In the latter case, we determined the value of P_{surf} as follows.

Figure 5 shows an example of the V_{step} vs. σ plot at -25.0 °C. The broken curve shows the result of the curve fitting using the hyperbolic tangent function, demonstrating the depletion of water vapor in the vicinity of a prism face. Then, the solid straight line, which was used for the determination of β, presents the tangential line of the hyperbolic tangent function at $\sigma = 0$, indicating V_{step} when there was no depletion of water vapor. In Fig. 5, when $\sigma = 0.046$, the broken curve exhibits the value of V_{step} = 0.40 μm/s, which is significantly smaller than the value of V_{step} on the solid straight line. This result demonstrates that due to the effect of the volume diffusion, the supersaturation at the crystal surfaces $(P_{surf} - P_e)/P_e$ decreased to 0.033,

which is the value of the horizontal axis of the solid straight line for $V_{step} = 0.40\,\mu$m/s. Therefore, from the relation on the solid straight line, P_{surf} can be obtained as

$$P_{surf} = \left(1 + \frac{V_{step}}{\beta}\right) P_e. \quad (5)$$

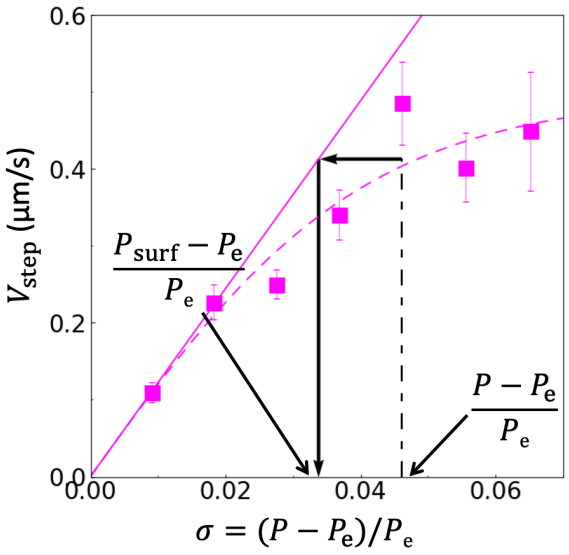


Fig. 5

Using the value of P_{surf}, we obtained $\Delta\mu_{surf} = k_B T \ln P_{surf}/P_e$. In Fig. 6, we summarized the relation between L and $1/\Delta\mu_{surf}$ under various T. Straight lines show the results of the curve fitting using eq. (4), demonstrating that the experimental data could be well fitted with eq. (4): elementary spiral steps on prism faces follow the BCF theory well.

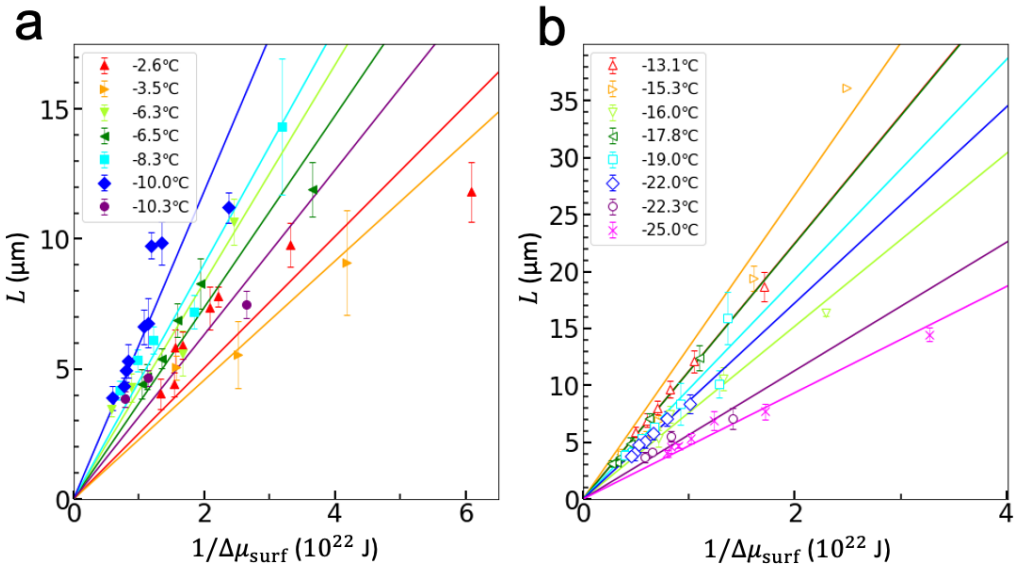


Fig. 6

In eq. (4), the only unknown parameter is κ. Hence, from the slopes of the straight lines in Fig. 6, we successfully obtained the values of κ as a function of T. Figure 7 shows the changes in κ, determined from Fig. 6, as a function of T. The value of κ (filled squares) on prism faces ranges from 1.5×10^{-10} to 8.5×10^{-10} J/m. A solid curve shows a guide for eyes. As shown in Fig. 7, κ reaches the peak at -15.3 °C. Although showing a large variation, κ decreases monotonically with increasing T from -15.3 to -2.6 °C and also with decreasing T from -15.3 to -26.0 °C.

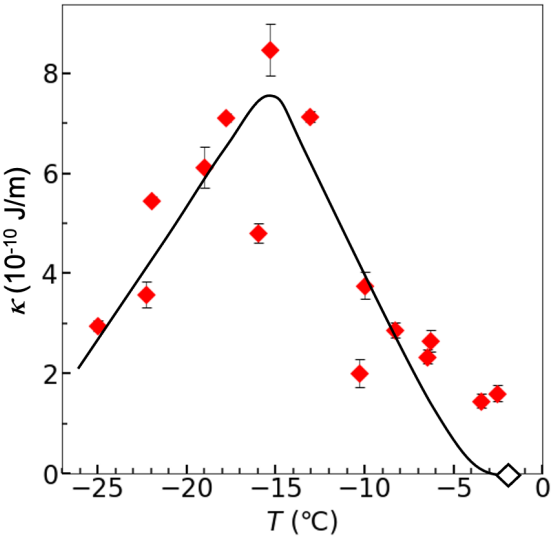


Fig. 7

There have existed so far two studies that determined κ of elementary spiral steps on basal faces of ice crystals. Inomata et al. determined κ on ice basal faces, on which screw dislocations were always located at the edges of ice crystals and L exhibited a significantly large variation.[24] On such basal faces, Inomata et al. obtained $\kappa = (5.0 \pm 1.9) \times 10^{-9}$ J/m from the $1/\Delta\mu_{\mathrm{surf}}$ dependence of L using eq. (4) at T from -13.0 to -3.2 °C, however when $T \leq$ -15.0 °C the data did not follow eq. (4). In contrast, Murata et al. determined κ on a basal face, on which screw dislocations were fortunately located in the interior of the basal face because of the coalescence of two neighboring ice crystals just before the observation.[40] On this basal face, L was uniform. There, Murata et al. obtained a more accurate value $\kappa = (4.7 \pm 0.2) \times 10^{-9}$ J/m at T from -

12.7 to -6.7 °C (in this T range temperature dependence of κ was not observed). Therefore, the value of κ obtained on prism faces is about 1/5 ~ 1/30 of that on basal faces. This result is qualitatively consistent with the previous study by Elbaum et al.[41] They found that the thermal roughening transition occurs on prism faces at $T \geq -2.0$ °C where κ becomes zero (the open square in Fig. 7), whereas basal faces are flat at the molecular level even at T just below 0 °C.[41] The presence and absence of the thermal roughening on prism and basal faces respectively indicate that κ on prism faces is smaller than that on basal faces.

The temperature dependence of κ on prism faces (Fig. 7) is peculiar when T < -15.3 °C. Because κ is a free energy composed of an enthalpy term (ΔH) and an entropy term ($-T\Delta S$), the monotonical decrease in κ with increasing T from -15.3 to -2.6 °C looks plausible. However, we cannot explain the increase in κ with increasing T from -25.0 to -15.3 °C at this moment. Recently, Llombart and coworkers carried out large-scale molecular dynamics calculation, and reported that step ledge free energy of a prism face shows the local maximum at temperatures around -20 °C.[42] They explained the presence of the local maximum utilizing the smoothening of a prism face through pre-melting. Because LCM-DIM cannot provide any direct information about surface structures, studies by GI diffractometry and SFG spectroscopy need to be performed in the future.

3.3. Temperature dependence of the morphology of ice crystals. As it is well known, Nakaya found that with decreasing temperature, snow crystals sequentially exhibit a hexagonal-plate shape (0 to -4 °C), a hexagonal-column shape (-4 to -10 °C), a hexagonal-plate shape (-10 to -22 °C), and a hexagonal-column shape (< -22 °C) (Fig. S4 in the supporting information).[43, 44] After this finding, five experimental studies tried to explain the

morphological change (summarized in Table S1). Hallet[45] and Kobayashi[46] measured the lateral velocity of macrosteps in air. In addition, Mason and coworkers[47] measured surface diffusion distance of water admolecules in air. However, these three studies performed the measurements only on basal faces and discussed the behavior on prism faces. To our knowledge, there have existed so far only two experimental studies that measured the T dependence of the growth kinetics on both basal and prism faces of ice crystals in vapor.[48, 49] Lamb and coworkers measured the normal growth rate R of basal and prism faces at T from -17 to -2 °C under a vacuum formed by a rotary pump. Although their macroscopic measurements exhibited a significant variation in R, their measurements reproduced the changes in the morphology with T.[48, 49] In addition, Kuroda and Lacmann tried to theoretically explain the morphological changes with T, assuming the differences in T of the thermal roughening transition and surface melting on basal and prism faces.[50] However, after the study by Kuroda and Lacmann, their assumptions were found to be incorrect (for details, see the caption of Fig. S4).[51-55] Therefore, the study on the mechanism of the morphological changes with temperature had returned to the starting point.

In this study, as shown in Fig. 4, the values of β on prism faces do not exceed those on basal faces at any T, indicating that the temperature dependence of β cannot explain the appearance of the hexagonal-plate shape. To explain the morphological changes with T, we further need to study the temperature dependence of the kinetics of normal growth rates R of prism and basal faces. Therefore, we calculated R at various σ and T, using the relation $R = V_{\mathrm{step}} \cdot (h/L)$:[30, 31] here h is the thickness of an elementary step (0.39 nm). However, as explained in detail in Fig. S5, we could not explain the morphological changes with T even taking into account R.

Why did our elementary-step-level measurements fail to explain the morphological changes with T? We suppose that the following two are the plausible reasons. One is the significant

variation in L on basal faces. Because of this variation, there existed temperatures at which L did not follow the picture of the BCF theory[36-38] (eq. (4)) in our previous study.[24] The variation in L is the intrinsic feature of basal faces, however at this moment we do not have a more appropriate theoretical model. Another is the difference in the background pressures. Lamb and Scott reported that the values of R under atmospheric pressure were about three orders of magnitude smaller than those under a vacuum formed by a rotary pump.[49] Our R (Fig. S5) measured under atmospheric pressure also shows the same tendency, probably resulting in the much smaller difference in R of basal and prism faces. Hence, to verify the changes in the crystal habit with T, we need to perform our observation at much higher σ under atmospheric pressure or at similar σ under vacuum conditions.

4. CONCLUSIONS

In this study, we successfully grew ice prism faces heteroepitaxially on the scratched $\{10\bar{1}0\}$ CdSe substrate. Then we observed individual elementary spiral steps on the ice prism faces by LCM-DIM. We measured lateral velocity of elementary spiral steps, V_{step}, as a function of supersaturation σ in the temperature (T) range from -25.0 to -2.6 °C. Then we obtained the following key findings.

(1) On ice prism faces, outcrops of screw dislocations are mostly located in the interiors of prism faces, whereas on basal faces screw dislocations are always located at the edges of crystals. In addition, on prism faces, the distance L between adjacent elementary spiral steps is uniform at constant σ and T, whereas on basal faces L exhibits a large variation even at constant σ and T.

(2) From the σ dependence of V_{step}, we determined the step kinetic coefficient β under various T. We found that on prism faces the value of β decreases monotonically with decreasing T from -2.6 to -25.0 °C, whereas on basal faces β shows a complicated behavior. Irrespective of T, the values of β on prism faces are significantly smaller than those on basal faces at the T range adopted in this study.

(3) From the $1/\Delta\mu_{surf}$ dependence of L, we evaluated the step ledge free energy κ on prism faces. We found that the value of κ on prism faces ranges from 1.5×10^{-10} to 8.5×10^{-10} J/m in the T range from -25.0 to -2.6 °C and reaches a peak at $T \sim$ -15 °C. These values are significantly smaller than those on basal faces (4.7 (±0.2) x 10^{-9} J/m)[40].

Acknowledgements

The authors thank Y. Saito, S. Kobayashi (Olympus Corporation) for technical support with LCM-DIM, and Y. Furukawa (Hokkaido University) for valuable discussions. G.S. is grateful for partial support from JSPS KAKENHI (Grant No. 19H02611).

ASSOCIATED CONTENT

Supporting information: The supporting information is available free of charge on the ACS Publication website at DOI: XXXXXXXXXX.

A schematic drawing of an observation chamber; LCM-DIM images of elementary spiral steps grown on an ice basal face at T = -15.0 °C and σ = 0.18: (a) 0 s, (b) 1.08 s, and (c) 2.15 s; distribution of distance L between adjacent elementary spiral steps; changes in morphology of snow crystals as functions of water vapor density and temperature; temperature dependence of the growth kinetics of normal growth rate R; time evolution of the lateral growth of an

elementary spiral step on an ice prism face at T = -6.3 °C and σ = 1.02; summary of previous experimental studies on the difference between the growth of basal and prism faces

Web-Enhanced Feature:

Time evolution of the lateral growth of elementary spiral steps on an ice prism face at T = -6.3 °C and σ = 0.02 (Video S1) is available as a video file in the HTML version of the paper.

References

(1) Pruppacher, H. R.; Klett, J. D., *Microphysics of Clouds and Precipitation*. Kluwer Academic Publishers: Dordrecht, 1997.
(2) Wallace, J. M.; Hobbs, P. V., Atmospheric Science: an Introductory Survey. In *International Geophysics Series*, 2nd ed.; Dmowska, R.; Hartmann, D.; Rossby, H. T., Eds. Academic Press: Amsterdam, 2006; Vol. 92.
(3) Benn, D.; D., E., *Glaciers and Glaciation*. Routledge: New York, 1998.
(4) Furukawa, Y.; Yamamoto, M.; Kuroda, T., Ellipsometric study of the transition layer on the surface of an ice crystal. *J. Cryst. Growth* **1987,** 82, 665-677.
(5) Furukawa, Y.; Kohata, S., Temperature dependence of the growth form of negative crystal in an ice single crystal and evaporation kinetics for its surfaces. *J. Cryst. Growth* **1993,** 129, 571-581.
(6) Raymond, J. A.; Wilson, P.; Devries, A. L., Inhibition of growth of nonbasal planes in ice by fish antifreezes. *Proc. Natl. Acad. Sci. U.S.A.* **1989,** 86, 881-885.
(7) Gonda, T.; Sei, T., The growth-mechanism of ice crytals grown in air at a low-pressure and their habit change with temperature. *Journal De Physique* **1987,** 48, 355-359.
(8) Sei, T.; Gonda, T., The growth mechanism and the habit change of ice crystals growing from the vapor-phase. *J. Cryst. Growth* **1989,** 94, 697-707.
(9) Sei, T.; Gonda, T., Growth rate of polyhedral ice crystals growing from the vapor-phase and their habit change. *Journal of the Meteorological Society of Japan* **1989,** 67, 495-502.
(10) Gonda, T.; Kakiuchi, H.; Moriya, K., In situ observation of internal structure in growing ice crystals by laser scattering tomography. *J. Cryst. Growth* **1990,** 102, 167-174.
(11) Gonda, T.; Arai, T.; Sei, T., Experimental study on the melting process of ice crystals just below the melting point. *Polar Meteorol. Glaciol.* **1999,** 13, 38-42.
(12) Sei, T.; Gonda, T.; Arima, Y., Growth rate and morphology of ice crystals growing in a solution of trehalose and water. *J. Cryst. Growth* **2002,** 240, 218-229.
(13) Gonda, T.; Sei, T., The inhibitory growth mechanism of saccharides on the growth of ice crystals from aqueous solutions. *Prog. Cryst. Growth Charact. Mater.* **2005,** 51, 70-80.
(14) Sei, T.; Gonda, T., Melting point of ice in aqueous saccharide solutions. *J. Cryst. Growth* **2006,** 293, 110-112.
(15) Furukawa, Y.; Shimada, W., Three-dimensional pattern formation during growth of ice dendrites -- its relation to universal law of dendritic growth. *J. Cryst. Growth* **1993,** 128, 234-239.
(16) Gonda, T.; Matsuura, Y.; Sei, T., In situ observation of vapor-grown ice crystals by laser two-beam interferometry. *J. Cryst. Growth* **1994,** 142, 171-176.

(17) Shimada, W.; Furukawa, Y., Pattern formation of ice crystals during free growth in supercooled water. *J. Phys. Chem. B* **1997,** 101, 6171-6173.
(18) Vorontsov, D. A.; Sazaki, G.; Hyon, S. H.; Matsumura, K.; Furukawa, Y., Antifreeze Effect of Carboxylated epsilon-Poly-L-lysine on the Growth Kinetics of Ice Crystals. *J. Phys. Chem. B* **2014,** 118, 10240-10249.
(19) Vorontsov, D. A.; Sazaki, G.; Titaeva, E. K.; Kim, E. L.; Bayer-Giraldi, M.; Furukawa, Y., Growth of Ice Crystals in the Presence of Type III Antifreeze Protein. *Crystal Growth & Design* **2018,** 18, 2563-2571.
(20) Bayer-Giraldi, M.; Sazaki, G.; Nagashima, K.; Kipfstuhl, S.; Vorontsov, D. A.; Furukawa, Y., Growth suppression of ice crystal basal face in the presence of a moderate ice-binding protein does not confer hyperactivity. *Proc. Natl. Acad. Sci. U.S.A.* **2018,** 115, 7479-7484.
(21) Sazaki, G.; Matsui, T.; Tsukamoto, K.; Usami, N.; Ujihara, T.; Fujiwara, K.; Nakajima, K., In situ observation of elementary growth steps on the surface of protein crystals by laser confocal microscopy. *J. Cryst. Growth* **2004,** 262, 536-542.
(22) Sazaki, G.; Zepeda, S.; Nakatsubo, S.; Yokoyama, E.; Furukawa, Y., Elementary steps at the surface of ice crystals visualized by advanced optical microscopy. *Proc. Natl. Acad. Sci. U.S.A.* **2010,** 107, 19702-19707.
(23) Sazaki, G.; Asakawa, H.; Nagashima, K.; Nakatsubo, S.; Furukawa, Y., Double spiral steps on I-h ice crystal surfaces grown from water vapor just below the melting point. *Cryst. Growth Des.* **2014,** 14, 2133-2137.
(24) Inomata, M.; Murata, K.-i.; Asakawa, H.; Nagashima, K.; Nakatsubo, S.; Furukawa, Y.; Sazaki, G., Temperature dependence of the growth kinetics of elementary spiral steps on ice basal faces grown from water vapor. *Cryst. Growth Des.* **2018,** 18, 786-793.
(25) Asakawa, H.; Sazaki, G.; Yokoyama, E.; Nagashima, K.; Nakatsubo, S.; Furukawa, Y., Roles of surface/volume diffusion in the growth kinetics of elementary spiral steps on ice basal faces grown from water vapor. *Cryst. Growth Des.* **2014,** 14, 3210-3220.
(26) Sazaki, G.; Inomata, M.; Asakawa, H.; Yokoyama, E.; Nakatsubo, S.; Murata, K.; Nagashima, K.; Furukawa, Y., In-situ optical microscopy observation of elementary steps on ice crystals grown in vapor and their growth kinetics. *Prog. Cryst. Growth Charact. Mater.* **2021,** 67, 1005500-1-11.
(27) Fukuta, N.; Mason, B. J., Epitaxial growth of ice on organic crystals. *J. Phys. Chem. Solids* **1963,** 24, 715-718.
(28) Reeber, R. R., Lattice-parameter and stoichiometric variations in CdSe. *J. Mater. Sci.* **1976,** 11, 590-591.
(29) Hobbs, P. V., *Ice Physics*. Clarendon Press: Oxford, 1974.
(30) Chernov, A. A., Modern Crystallography III. In *Springer Ser. Solid-State Sci.*, Cardona, M.; Fulder, P.; Queisser, H.-J., Eds. Springer-Verlag: Berlin, 1984; Vol. 36.
(31) Markov, I. V., *Crystal Growth for Beginners*. World Scientific Publishing: Singapore, 1995.
(32) Rossini, F. D.; Wag, A., D.D.; Evans, W. H.; Levine, S.; Jaffe, I., Selected values of chemical thermodynamic properties. *National Bureau of Standards (U.S,) Circular* **1952,** 500, 126-128.
(33) Hall, W. D.; Pruppacher, H. R., Survival of ice particles falling from cirrus clouds in subsaturated air. *Journal of the Atmospheric Sciences* **1976,** 33, 1995-2006.
(34) Sonntag, D., Important new Values of the Physical Constants of 1986, Vapour Pressure Formulations based on the ITS-90, and Psychrometer Formulae. *Z. Meteorol.* **1990,** 70, 340-344.

(35) Murphy, D. M.; Koop, T., Review of the vapour pressures of ice and supercooled water for atmospheric applications. *Quarterly Journal of the Royal Meteorological Society* **2005,** 131, 1539-1565.
(36) Frank, F. C., The influence of dislocations on crystal grwoth. *Discuss. Faraday Soc.* **1949,** 5, 48-54.
(37) Burton, W. K.; Cabrera, N.; Frank, F. C., Role of dislocations in crystal growth. *Nature* **1949,** 163, 398-399.
(38) Burton, W. K.; Cabrera, N.; Frank, F. C., The growth of crystals and the equilibrium structure of their surfaces. *Phil. Trans. Roy. Soc. London Series a-Math. Phys. Sci.* **1951,** 243, 299-358.
(39) Cabrera, N.; Levine, M. M., On the dislocation theory of evaporation of crystals. *Philos. Mag.* **1956,** 1, 450-458.
(40) Murata, K.; Nagashima, K.; Sazaki, G., In situ observations of spiral growth on ice crystal surfaces. *Phys. Rev. Mater.* **2018,** 2, 093402-1-7.
(41) Elbaum, M.; Lipson, S. G.; Dash, J. G., Optical study of surface melting on ice. *J. Cryst. Growth* **1993,** 129, 491-505.
(42) Llombart, P.; Noya, E. G.; MacDowell, L. G., Surface phase transitions and crystal habits of ice in the atmosphere. *Science Advances* **2020,** 6, eaay9322-1-9.
(43) Nakaya, U., *Snow Crystals, Natural and Artificial*. Harvard Univ. Press: Cambridge, 1954.
(44) Kobayashi, T., The growth of snow crystals at low supersaturations. *Philos. Mag.* **1961,** 6, 1363-1370.
(45) Hallett, J., The growth of ice crystals on freshly cleaved covellite surfaces. *Philos. Mag.* **1961,** 6, 1073-1087.
(46) Kobayashi, T., On the variation of ice crystal habit with temperature. *Physics of Snow and Ice* **1967,** 1, 95-104.
(47) Mason, B. J.; Bryant, G. W.; Vandenheuvel, A. P., The growth habits and surface structure of ice crystals. *Philos. Mag.* **1963,** 8, 505-526.
(48) Lamb, D.; Hobbs, P. V., Growth rates and habits of ice crystals grown from vapor phase. *J. Atmos. Sci.* **1971,** 28, 1506-1509.
(49) Lamb, D.; Scott, W. D., Linear growth-rates of ice crystals grown from vapor-phase. *J. Cryst. Growth* **1972,** 12, 21-31.
(50) Kuroda, T.; Lacmann, R., Growth kinetics of ice from the vapor phase and its growth forms. *J. Cryst. Growth* **1982,** 56, 189-205.
(51) Elbaum, M., Roughening transition observed on the prism facet of ice. *Phys. Rev. Lett.* **1991,** 67, 2982-2985.
(52) Sazaki, G.; Zepeda, S.; Nakatsubo, S.; Yokomine, M.; Furukawa, Y., Quasi-liquid layers on ice crystal surfaces are made up of two different phases. *Proc. Natl. Acad. Sci. U.S.A.* **2012,** 109, 1052-1055.
(53) Asakawa, H.; Sazaki, G.; Nagashima, K.; Nakatsubo, S.; Furukawa, Y., Prism and other high-index faces of ice crystals exhibit two types of quasi-liquid layers. *Cryst. Growth Des.* **2015,** 15, 3339-3344.
(54) Asakawa, H.; Sazaki, G.; Nagashima, K.; Nakatsubo, S.; Furukawa, Y., Two types of quasi-liquid layers on ice crystals are formed kinetically. *Proc. Natl. Acad. Sci. U.S.A.* **2016,** 113, 1749-1753.
(55) Murata, K.; Asakawa, H.; Nagashima, K.; Furukawa, Y.; Sazaki, G., Thermodynamic origin of surface melting on ice crystals. *Proc. Natl. Acad. Sci. U.S.A.* **2016,** 113, E6741-E6748.

Figure Captions

Fig. 1. Photomicrographs of a $\{10\bar{1}0\}$ CdSe substrate 10 min. after water vapor in the observation chamber became supersaturated. Panels (a) and (b) show a low-magnification image and a high-magnification image in the area marked by the dotted rectangle in (a), respectively. White and black arrowheads indicate scratches that were intentionally made, using a glass cutter, just before and 7-days before the experiment. 46% ice crystals formed on the new scratches showed a rectangular shape and the same orientation, as the crystal marked by the black arrow. The white arrow in (a) presents only the ice crystal formed on the 7-days-old scratch. Although the ice crystal marked by the white dotted arrow appeared as if it was formed on the 7-days-old scratch (marked by the black arrowhead), time evolution images revealed that this crystal was formed on another small scratch whose history was unknown. Hence, this crystal was excluded from the discussion in the main text. T = -13.3 °C and σ = 0.20 (P = 232 Pa and P_e = 193 Pa).

Fig. 2. LCM-DIM images of elementary spiral steps grown on an ice prism face at T = -6.3 °C and σ = 0.02 (P = 366 Pa and P_e = 359 Pa): (a) 0 s, (b) 5.5 s, (c) 11.0 s, and (d) 16.4 s. A black arrowhead presents the location of a screw dislocation. On prism faces, screw dislocations were mostly located in the interiors of crystal faces. Distance L between adjacent spiral steps on prism faces was almost uniform. The velocity V_{step} of elementary spiral steps was determined from the time evolution of the position of an identical step (marked by white arrowheads). A movie of the process A-D is available as Video S1.

Fig. 3. Changes in V_{step} of ice prism faces as a function of σ. (a) Temperature T: -2.6 (▲), -3.5 (▶), -6.3 (▼), -6.5 (◀), -8.3 (■), -10.0 (◆) and -10.3 (●) °C. (b) Temperature T: -13.1 (△), -15.3 (▷), -16.0 (▽), -17.8 (◁), -19.0 (□), -22.0 (◇), -22.3 (○) and -25.0 (×) °C. Solid straight lines show the results of the curve fittings using a linear function from the origin. When the depletion of water vapor was formed in the vicinity of a growing prism face, the V_{step} vs. σ plot

deviated from the linear relation and was finally saturated with increasing σ (T = -22.0, -22.3 and -25.0 °C). Broken curves show the results of the curve fittings using a hyperbolic tangent function.

Fig. 4. Temperature dependence of the step kinetic coefficient β determined newly on prism faces in this study (filled squares) and that on basal faces determined previously[24] (open circles). Panels (a) and (b) present a β vs. T plot and an lnβ vs. 1000/T plot, respectively. In panel (b), a straight line presents the result of the curve fitting using eq. (2), showing $\Delta G \sim 44$ kJ/mol.

Fig. 5. An example of changes in V_{step} on a prism face as a function σ at T = -25.0 °C. The solid straight line presents V_{step} when there was no depletion of water vapor in the vicinity of the prism face. The broken curve shows the result of the curve fitting using a hyperbolic tangent function. For the derivation of P_{surf} from this figure, see the main text.

Fig. 6. Changes in L on prism faces as a function of $1/\Delta\mu_{surf}$. (a) Temperature T: -2.6 (▲), -3.5 (▶), -6.3 (▼), -6.5 (◀), -8.3 (■), -10.0 (◆) and -10.3 (●) °C. (b) Temperature T: -13.1 (△), -15.3 (▷), -16.0 (▽), -17.8 (◁), -19.0 (□), -22.0 (◇), -22.3 (○) and -25.0 (×) °C. Solid straight lines show the results of the curve fitting using eq. (4).

Fig. 7. Changes in the step ledge free energy κ on prism faces as a function of T. Filled squares show κ obtained from Fig. 6. The open square represents κ = 0 J/m when $T \geq$ -2 °C because of the thermal roughening transition of prism faces.[41] A solid curve shows a guide for eyes.

AUTHOR INFORMATION

Corresponding Author

Prof. Gen Sazaki: Institute of Low Temperature Science, Hokkaido University, N19-W8, Kita-ku, Sapporo 060-0819, Japan. E-mail: sazaki@lowtem.hokudai.ac.jp.

Phone and fax: +81-11-706-6880

Author Contributions

G.M., K.M., K.N., and G.S. designed the research performed by G.M. and G.S. A.K. found the heteroepitaxial growth of prism faces of ice crystals on a $\{10\bar{1}0\}$ CdSe substrate. G.M. and G.S. wrote the paper. The authors declare no conflict of interest. All authors have approved the final version of the manuscript.

Funding Sources

JSPS KAKENHI (No. 19H02611).

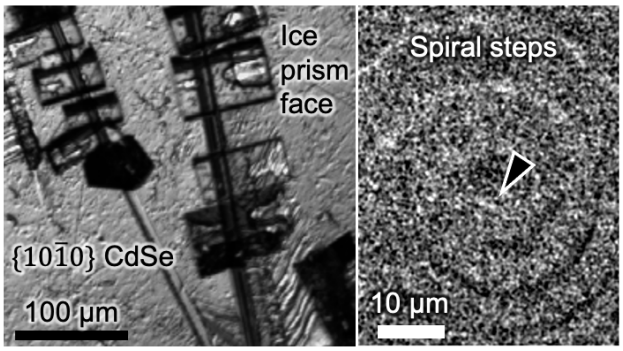
ABBREVIATIONS

LCM-DIM: laser confocal microscopy combined with differential interference contrast microscopy

For Table of Contents Use Only

Growth kinetics of elementary spiral steps on ice prism faces grown in vapor and their temperature dependence

Genki Miyamoto, Akira Kouchi, Ken-ichiro Murata, Ken Nagashima, Gen Sazaki



Synopsis (58 words ≤ 60 words)

We grew ice prism faces heteroepitaxially on a {10$\bar{1}$0} CdSe wafer and measured lateral velocity of elementary spiral steps on prism faces, for the first time, by advanced optical microscopy. We determined dependence of a step kinetic coefficient β on temperature (from -25.0 to -2.6 °C) and found that the value of β decreases monotonically with decreasing temperature.